Eur. Phys. J. Appl. Phys. (2016) 75: 24712
DOI: 10.1051/epjap/2016150564

THE EUROPEAN PHYSICAL JOURNAL APPLIED PHYSICS

Regular Article

The plasma footprint of an atmospheric pressure plasma jet on a flat polymer substrate and its relation to surface treatment*

Iuliia Onyshchenko[a], Anton Yu. Nikiforov, Nathalie De Geyter, and Rino Morent

Research Unit Plasma Technology (RUPT), Department of Applied Physics, Faculty of Engineering and Architecture, Ghent University, Sint-Pietersnieuwstraat 41, 9000 Ghent, Belgium

Received: 19 November 2015 / Received in final form: 26 February 2016 / Accepted: 9 May 2016

Abstract. The aim of this work is to show the correlation between the plasma propagation in the footprint of an atmospheric pressure plasma jet on a flat polymer surface and the plasma treatment impact on the polymer properties. An argon plasma jet working in open air is used as plasma source, while PET thin films are used a substrates for plasma treatment. Light emission photographs are taken with an ICCD camera to have a close look at the generated structures in the plasma jet footprint on the surface. Water contact angle (WCA) measurement and X-ray photoelectron spectroscopy (XPS) analysis are also performed to obtain information about the impact of the plasma treatment on the PET surface characteristics. A variation in ICCD camera gate duration (1 μs, 100 μs, 50 ms) results in the photographs of the different plasma structures occurring during the plasma propagation on the flat PET surface. Contact angle measurements provide results on improvement of the PET hydrophilic character, while XPS analysis shows the distribution of atomic elements on the treated substrate surface. Light emission images help explaining the obtained WCA and XPS results.

1 Introduction

The increasing amount of publications about atmospheric pressure plasma jets in the last decade indicates the growing interest in this type of plasma source. Scientific researchers around the world work on different aspects: applications [1,2], modelling [3], new design [4], experimental work [5], etc. Benefits such as low temperature, no need for vacuum equipment, high flexibility, simple construction, rich plasma chemistry, no limitation to the sample size and curvature, good treatment capability give atmospheric pressure plasma jets their excellent reputation. Among the different successful applications, plasma jets are also very effective in high-quality surface processing of the top layers of material while all bulk properties remain unchanged. This effect together with a remarkable plasma jet penetration in small-size constructions [6] allows using atmospheric plasma jets for a gentle treatment of 3D structures [7].

A large amount of atmospheric pressure plasma jet applications can be found in many research areas: chemistry, materials, biochemistry, physics and different fields in medicine [8,9]. Despite the tremendous mass of studies that has been done on plasma jet sources, many questions remain unanswered. For plasma diagnostics and characterizations, the following techniques have been applied: probes, optical emission spectroscopy, absorption spectroscopy, mass spectroscopy and scattering [10,11]. One of the other applied options for a fast analysis of plasma processes occurring in atmospheric pressure plasma jets is taking high time resolved ICCD camera photographs to investigate the plasma evolution in space and time. This procedure helped to discover the non-continuous discharge mode in the plasma jet. It appears to include many separated ignitions of plasma forms called "bullets". However, despite these discoveries, there are still many dark corners in the field of atmospheric pressure plasmas such as theoretical explanations, modeling computations and missing experimental work [12,13].

The purpose of this study is to investigate the plasma propagation in the footprint of an atmospheric pressure plasma jet on a flat polymer sample. By using an ICCD camera with different exposure times, it is possible to show the plasma jet transfiguration. The timing range should be big enough to observe the difference in formations behavior and make the proper deductions. Apart from ICCD camera imaging investigations, additional measurements of wettability and atomic element concentration on plasma-treated polymer samples are also performed.

[a] e-mail: Iuliia.Onyshchenko@UGent.be

* Contribution to the topical issue "6th Central European Symposium on Plasma Chemistry (CESPC-6)", edited by Nicolas Gherardi, Ester Marotta and Cristina Paradisi

Conclusions made based on the plasma jet footprint photographs should help to explain the observed plasma treatment effects.

2 Experimental

2.1 Atmospheric pressure plasma jet

This work is focused on the representation of the atmospheric pressure plasma jet footprint on a flat polymer sample. The schematic illustration of the used experimental plasma jet set-up is presented in Figure 1 and is similar to the plasma source used in previous work [6]. A quartz capillary with inside and outside diameters of 1.3 mm and 3.0 mm respectively determines the volume of the generated discharge. A tungsten wire (diameter equal to 0.5 mm) with a half-sphere shaped tip is placed inside the capillary and used as high voltage electrode. A 10 mm wide second ring-shaped ground electrode is placed outside the capillary at a distance of 35 mm from the high-voltage electrode and 20 mm away from the edge of the capillary. High purity argon at a constant flow rate of 1 standard litre per minute (SLM) fills the capillary. Applying a high voltage to the tungsten wire provides the ignition of a plasma in the inter-electrode gap. Moreover, a long outflowing plasma (so-called effluent) propagation appears in the surrounding air. In this work, the power supply is set to produce an AC high voltage at a fixed frequency of 60 kHz and a fixed amplitude of 7 kV (peak-to-peak). This applied voltage value has been measured with a high voltage probe (Tektronix P6015A) connected to the tungsten wire. A current transformer (Pearson Current Monitor Model 2877) has also been used to obtain the discharge current. The acquired voltage-current waveforms have been recorded using a Picoscope 3204A digital oscilloscope. Based on the derived data, the average power of the discharge has been calculated. For the experimental parameters used in this work, the discharge power has been determined and was found to be 3.1 W. Figure 2 shows a typical voltage and current waveform of the plasma jet. Current peaks indicate the discharge ignition.

Polyethylene terephthalate (PET) flat samples (250 μm thickness, Goodfellow, Germany) have been used to show the efficiency of the plasma jet treatment. Substrates have been placed without any pre-treatment 2 mm below the edge of the capillary and have been exposed to the plasma jet for the 40 s. During the treatment process, the sample and the plasma jet have been permanently fixed at the above mentioned capillary-sample distance (2 mm). In this way, a single plasma treatment spot is produced on the exposed PET samples.

2.2 Light emission images

Discharge images have been taken by a Hamamatsu ICCD camera (model C8484). The camera is equipped with a UV-VIS-IR CoastalOprR lens F/4-F/45 60 mm Macro.

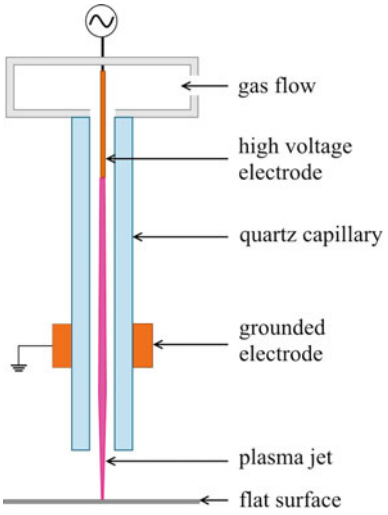

Fig. 1. Schematic diagram of the experimental atmospheric pressure plasma jet set-up.

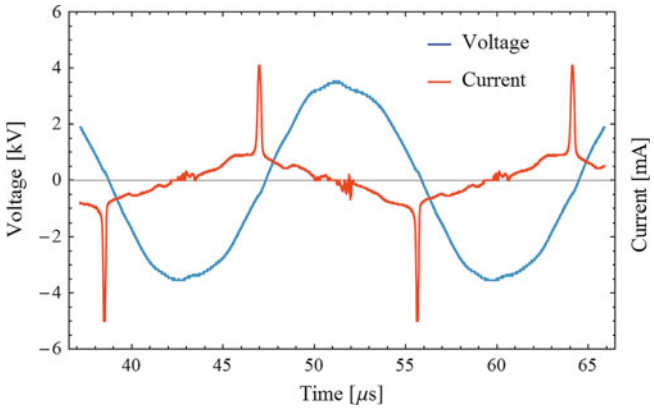

Fig. 2. Voltage and current waveforms of the plasma jet.

The ICCD camera exposure time has been set to 1 μs, 100 μs and 50 ms. These values allow to obtain different structures of the atmospheric pressure plasma jet since the discharge period is 16×10^{-6} s. Thus, the obtained images cover the most relevant examples of plasma jet features: time-integrated images and single-ignited discharges. The images of plasma propagations have been recorded without the use of any filter. Therefore, the whole spectral range of ICCD from 290 to 900 nm has been used.

2.3 Water contact angle measurements

Water contact angle (WCA) measurements give the opportunity to evaluate the plasma treatment effect on the surface free energy of a polymer surface which is an essential surface parameter. A commercial Krüss Easy Drop optical system (Krüss GmbH, Germany) has been used to obtain the WCA values on the plasma treated samples. Measurements are performed in an ambient air at room temperature immediately after the plasma exposure. An exact volume (1 μL) of distilled water is released by a high precision liquid dispenser and subsequently placed

on the treated substrate. The interline CCD video camera records and stores the drop image using PC-based acquisition and data processing. By using computer software provided with the instrument, the measurements of the static contact angles values are fully automated. The values of the static contact angles are obtained using Laplace-Young curve fitting based on the imaged sessile water drop profile. Each water contact angle measurement reported in this paper has an estimated error of less than 2.0° with 95% probability.

2.4 X-ray photoelectron spectroscopy

The chemical composition of the plasma-treated PET samples is obtained by X-ray photoelectron spectroscopy (XPS). XPS survey spectra are recorded with a PHI Versaprobe II spectrometer. A monochromatic Al K_α X-ray source ($h\nu$ = 1486.6 eV) operating at 50 W is employed. Survey scans are recorded in a vacuum of at least 10^{-6} Pa with a pass energy of 187.85 eV in steps of 0.8 eV at a take-off angle of 45° relative to the sample surface. The obtained XPS survey scans are subsequently processed using Multipak (9.5) software to determine the elemental composition at the surface of the samples from the peak area ratios.

3 Results and discussion

3.1 Light emission images

As was reported in previous work [14], there is no complete correlation between the cross-section of the plasma jet footprint noticed with the naked eye and the real effectively treated area on the sample. Therefore, a close look at the plasma treatment process is required. To gain more information about plasma propagation in the lateral direction on a flat polymer sample, high-quality photographs have been taken using an ICCD camera.

Pulsations on the current waveforms on Figure 2 represent the "birth" and "death" of plasma discharges. There are some works [9,12,15,16] where such separated single discharge is called "bullet". Nevertheless, the lifetime of the bullet is very short (few μs) and the timing between each of the passing set is also small. Together with the continuing process, this effect gives the naked eye the false picture of the integrated model without the bullet structure of the plasma jet.

The photographs presented in Figure 3 show the different structures of the atmospheric pressure plasma jet footprint on the flat polymer surface depending on the exposure time of the ICCD camera. Yellow lines illustrate the inner tube form. The distance between the capillary edge and the surface is 2 mm for all figures. Namely the best resolution of the plasma structures on the surface is recognized on Figure 3a for the 1 μs ICCD camera exposure time. This image was selected from a set of photos taken in a row each μs. Since each bullet passes the distance on its way, the camera records a different image each

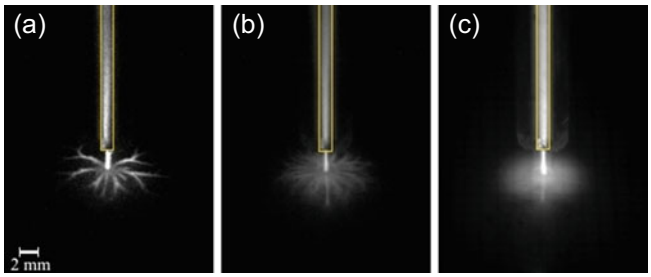

Fig. 3. ICCD images of the plasma jet footprint on a flat polymer surface with different exposure times: (a) 1 μs, (b) 100 μs and (c) 50 ms.

time. Figure 3a shows that the structure has independent "branches" which propagate from the center in radial direction. Each branch has a few bifurcations that separate into two smaller parts at the end of the branch. The thickness changes from thick central parts to thin ends. Nevertheless, most part of each section looks uniformly thick. There are approximately 8–10 main branches propagating on the surface from the central point where the plasma jet is directed. The radial propagation length of the majority of the structure parts is about 6 mm. This size should not be read as a precise value since the camera sensitivity and noise level make the thin and less bright structure ends vanish. It is only given as an indicative value.

Figure 3b demonstrates the photograph of the plasma jet recorded by the ICCD camera within a 100 μs timing. It can be seen that the branch structure is not so obvious as the one presented on the previous image taken with an exposure time of 1 μs. A set of thin, weak lines is however still observed. Although the line number is much greater than for the shorter exposure time, the lines look thinner and cover a larger area close to the center of the plasma jet footprint. Since the camera gap has been opened to 100 μs, the ICCD camera records several single bullets and thus different branched structures on the polymer surface. All these branches overlap each other thereby creating the combined image presented in Figure 3b. Each recorded frame has a different image, in other words, each photo represents a different combination of the plasma jet branched structures on the surface. The propagation radius on the surface is approximately 3.7 mm, which is smaller than the radius which has been observed for a photograph taken with a 1 μs exposure time. This conclusion is based only on a visual comparison of photos taken by the ICCD camera used in this work.

The most uniform glow is observed on Figure 3c which shows a photograph taken with a 50 ms exposure time. The explanation of the observed effect is the following: during the time when the camera gate is open, the ICCD camera records so many single discharges and thus so many different branched structures that they cover all space resulting in a homogenous glow on the polymer surface. Because 50 ms is a long integration time, recorded images are the same each time hence this integration time is too high to still observe the difference between separated

discharges and thus creates the impression of a continuous plasma glow. Moreover, the radius of the plasma jet footprint is about 3 mm which is twice less than for the 1 μs image and also still considerably smaller than for the 100 μs photograph. Since the ends of the plasma branches on the surface are thin, only appear for a very short time at different positions and almost never overlap, the photograph in Figure 3c does not show the plasma discharge propagation at a long distance from the plasma jet center. However this result is strongly related to the quality of the ICCD camera that was used in this work and the sizes of light emitting plasma footprint can be compared only for photos that were taken with the same camera parameters.

3.2 Static water contact angle measurements

The surface free energy is one of the most important characteristics of any polymer material. The higher the surface free energy is, the lower the WCA value and the higher the surface hydrophilicity is. WCA measurements on a plasma treated PET sample have been performed to investigate the effect of plasma treatment on the surface hydrophilicity. Flat squared (3 × 3 cm) PET samples have been exposed to the plasma effluent for 40 s. During the experiment, the distance between the end of the capillary and the sample is maintained at 2 mm. Although the plasma jet itself is directed at one single point on the sample, the plasma causes an effective surface modification in a much larger circle-shaped area as shown in Figure 4. This figure presents the WCA profile observed along a straight line through the center of the treated zone. To obtain a spatial resolution of about 1 mm at least 5 samples were measured in different positions: water droplets were placed as close as possible to each other on the substrate with small shift for the first droplet on every sample. In the end result the combination of all measurements gives the profile of WCA each millimeter.

It is important to note that the distance "0 mm" represents the exact position of the plasma jet and that the two red lines mark the active plasma jet zone, which is equal to 1 mm in the case of the plasma parameters used to obtain Figure 4. In addition, the horizontal axis crosses the vertical axis at a WCA value of 87°, which is the average WCA value of the untreated PET sample. Following the measurement technique described in previous work [14], WCA results with a high spatial resolution have been obtained in Figure 4. This figure shows a substantial improvement in the hydrophilic characteristics of the plasma treated surface in an area with a radius of more than 10 mm. A minimum WCA value of approximately 22° is observed in the center of treated area. Moving further away from the center results in a gradual increase in WCA value until a constant WCA value slightly below the WCA value of the untreated sample is reached. In a radius of approximately 8 mm, the WCA values are more than 50% lower than the value of the untreated sample, which is still higher than the largest recorded propagation length (approximately 6 mm for the 1 μs photograph).

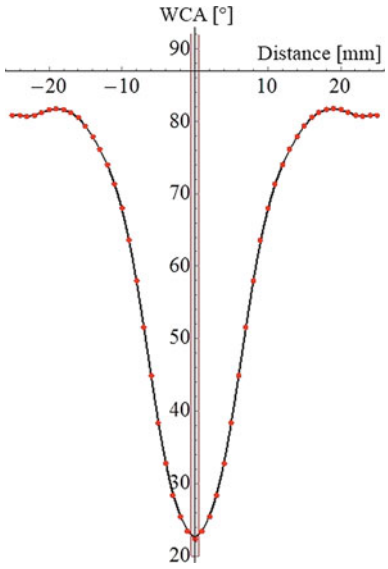

Fig. 4. WCA profile on a plasma-treated PET sample.

Based on the ICCD photographs shown above, the curve of the WCA profile can be explained as following. First of all, the branched plasma jet structures on the polymer surface are not permanent in time. Therefore, during the exposure time, plasma branches move around the center point and provide a roughly uniform treatment at an equal radial distance. On the other hand, the concentration of branched structures and their thickness vary from highly concentrated thick parts in the center to low concentrated thin ends at the edge. Thus, the central part is mostly uniformly covered with reactive plasma species during the complete treatment process. This impact produces the highly effective modification in the central sample part. On the contrary, the edges of the plasma jet footprint structures are quite thin and lie far away from each other. This situation together with their low appearance frequency result in a short interaction time between the sample surface and reactive plasma species. For this reason, the observed treatment effect is less pronounced at distances further away from the central point. The difference in radii of effectively treated area based on WCA measurements and the light emitting plasma region is due to the quality of ICCD camera. The propagation of plasma brunches should be farther but since the ends of this structure are thin and their emitted light is weak, the sensitivity of camera that was used in this work is not enough to capture them.

3.3 XPS results

Besides WCA measurements, XPS analysis has also been performed to obtain information about the chemical composition of the treated PET surface and to correlate these results with the WCA measurements. Low resolution XPS survey scans have been acquired to determine the atomic composition of the sample surface. To have comparable results, XPS analysis has been performed at the same

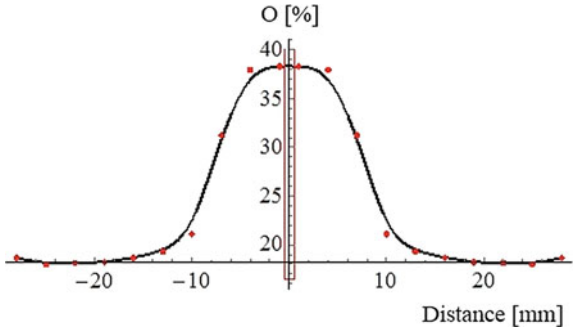

Fig. 5. Oxygen concentration on a plasma-treated PET sample.

positions on the treated PET sample as during the WCA measurements. Figure 5 shows the oxygen concentration on the treated surface along a diagonal line crossing the center of plasma jet footprint. Similar to Figure 4, the distance "0 mm" represents the exact position of the plasma jet and that the two red lines mark the active plasma jet zone. The horizontal axis crosses the vertical axis at 18.2% of oxygen, which is the oxygen atomic concentration present on the untreated PET surface. The highest amount of incorporated oxygen is observed in the center of the analyzed line – about 38%. Moving away from the center, the amount of incorporated oxygen gradually decreases until an oxygen concentration close to the untreated sample is found. In a region with a radius of approximately 10 mm, a high amount of incorporated oxygen is observed. The oxygen curve, after mirror reflection along the horizontal axis, has a shape quite similar to the WCA results presented in Figure 4. This means that oxygen incorporation on the treated surface is responsible for the larger surface free energy or sample hydrophilicity. The oxygen profile shape can be explained in the same way as was done in the previous section for WCA measurements.

4 Conclusion

The main results of this work demonstrate the interrelation between the plasma treatment efficiency and detailed images of the plasma jet footprint on a flat PET surface. By using an ICCD camera, light emission photographs of the argon plasma jet working in open air have been taken with different exposure times. A camera exposure time of 1 μs recorded images with highly resolved structures in the plasma jet footprint on flat samples similar to tree branches. With increasing camera gate timing, these branched structures started to vanish and completely disappear at the highest exposure time. This observation has been explained by thin edges on the branch ends and their variety in appearance locations. WCA measurements and XPS analysis have also been carried out on the PET substrate to obtain information about the plasma treatment efficiency. WCA results show a highly hydrophilic area in the center of the plasma-treated region. This effect has been explained by the obtained light emission images: in the central part of the plasma jet footprint the concentration of excited plasma species is higher than farther away from the center. XPS analysis of the plasma-treated substrate gave results similar to the WCA measurements and additionally confirmed the significance of detailed analysis of plasma jet footprints with light emission images.

The research leading to these results has received funding from the European Research Council under the European Union's Seventh Framework Program (FP/2007-2013)/ERC Grant Agreement No. 279022.

References

1. M. Laroussi, T. Akan, Plasma Processes Polym. **4**, 777 (2007)
2. A. Schutze, J.Y. Jeong, S.E. Babayan, J. Park, G.S. Selwyn, R.F. Hicks, IEEE Trans. Plasma Sci. **26**, 1685 (1998)
3. Y. Bartosiewicz, P. Proulx, Y. Mercadier, J. Phys. D: Appl. Phys. **35**, 2139 (2002)
4. C.C. Hsu, Y.J. Yang, IEEE Trans. Plasma Sci. **38**, 496 (2010)
5. N. Mericam-Bourdet, M. Laroussi, A. Begum, E. Karakas, J. Phys. D: Appl. Phys. **42**, 7 (2009)
6. I. Onyshchenko, N. De Geyter, A.Y. Nikiforov, R. Morent, Plasma Processes Polym. **12**, 271 (2015)
7. A. Lehmann, A. Rueppell, A. Schindler, I.M. Zylla, H.J. Seifert, F. Nothdurft, M. Hannig, S. Rupf, Plasma Processes Polym. **10**, 262 (2013)
8. J.F. Kolb, A.A.H. Mohamed, R.O. Price, R.J. Swanson, A. Bowman, R.L. Chiavarini, M. Stacey, K.H. Schoenbach, Appl. Phys. Lett. **92**, 3 (2008)
9. J.L. Walsh, F. Iza, N.B. Janson, V.J. Law, M.G. Kong, J. Phys. D: Appl. Phys. **43**, 14 (2010)
10. S. Pellerin, J.M. Cormier, F. Richard, K. Musiol, J. Chapelle, J. Phys. D: Appl. Phys. **29**, 726 (1996)
11. S. Hofmann, A.F.H. van Gessel, T. Verreycken, P. Bruggeman, Plasma Source. Sci. Technol. **20**, 12 (2011)
12. N. Puač, D. Maletić, S. Lazović, G. Malović, A. Đorđević, Z.L. Petrović, Appl. Phys. Lett. **101**, 024103 (2012)
13. O. Guaitella, A. Sobota, J. Phys. D: Appl. Phys. **48**, 12 (2015)
14. I. Onyshchenko, A.Y. Nikiforov, N. De Geyter, R. Morent, Plasma Processes Polym. **12**, 466 (2015)
15. J.L. Walsh, M.G. Kong, IEEE Trans. Plasma Sci. **39**, 2306 (2011)
16. S. Wu, H. Xu, Y. Xian, Y. Lu, X. Lu, AIP Adv. **5**, 7 (2015)